

000 001 TEAM, THEN TRIM: AN ASSEMBLY-LINE LLM 002 FRAMEWORK FOR HIGH-QUALITY TABULAR DATA 003 GENERATION 004 005

006 **Anonymous authors**
007 Paper under double-blind review
008
009
010
011

ABSTRACT

013 While tabular data is fundamental to many real-world machine learning (ML) ap-
014 plications, acquiring high-quality tabular data is usually labor-intensive and ex-
015 pensive. Limited by the scarcity of observations, tabular datasets often exhibit
016 critical deficiencies, such as class imbalance, selection bias and low fidelity. To
017 address these challenges, building on recent advances in Large Language Models
018 (LLMs), this paper introduces team-then-trim, a framework that synthesizes high-
019 quality tabular data through a collaborative team of LLMs, followed by a rigorous
020 data quality control (QC) pipeline. In our framework, tabular data generation is
021 conceptualized as a manufacturing process: specialized LLMs, guided by domain
022 knowledge, are tasked with generating different data components sequentially, and
023 the resulting products, i.e., the synthetic data, are systematically evaluated across
024 multiple dimensions of QC. Empirical results on both simulated and real-world
025 datasets demonstrate that our framework outperforms the state-of-the-art methods
026 in producing high-quality tabular data, highlighting its potential to support down-
027 stream models when direct data collection is practically infeasible.
028

1 INTRODUCTION

030 Machine learning (ML) systems in domains like healthcare (Provost & Murray, 2022), transpor-
031 tation (Washington et al., 2020), and the social sciences (Aneshensel, 2012) depend heavily on tabular
032 datasets. According to uniform convergence theorems and generalization bounds in classical statis-
033 tical learning theory (Feldman & Vondrak, 2018), if we can sample a sufficiently large number of
034 tabular data points from the underlying space, we can reliably train predictive models that generalize
035 well and achieve accurate performance. In practice, however, we often have to begin with a tabular
036 dataset sampled from the true data distribution, which is typically small and may suffer from various
037 deficiencies, such as bias (Little & Rubin, 2019), imbalance (Thabtah et al., 2020) and noise (Gupta
038 & Gupta, 2019). For example, in medical studies of diseases such as type-I diabetes, patients may
039 constitute only a small minority compared to non-patient participants, while all of them are at some
040 level of risk as indicated by the screening results. Under such data imbalance, downstream mod-
041 els trained solely on a limited original dataset often struggle to capture the true decision boundary,
042 leading to biased predictions, poor generalization to minority groups, and reduced robustness(Chen
043 et al., 2023). If we can generate high-quality data that are plausible under domain constraints and di-
044 verse enough to cover rare or unseen configurations, the accuracy and robustness of the downstream
045 models can be improved without costly data collection.

046 However, traditional data generation methods, such as resampling (e.g., SMOTE (Chawla et al.,
047 2002)) can only extrapolate from observed samples. While effective within the boundaries of the
048 original data, they remain constrained in exploration, often reinforcing the same biases and failing
049 to recover rare or missing subpopulations (Li & Vasconcelos, 2019). Deep generative models, e.g.,
050 CTGAN, TVAE (Xu et al., 2019), although more expressive, typically demand substantial amounts
051 of data and struggle in low-data regimes where augmentation is most needed. More recently, Large
052 Language Models (LLMs) have emerged as a new paradigm for data generation, leveraging broad
053 world knowledge and few-shot reasoning abilities (Seedat et al., 2023; Patel et al., 2024). How-
054 ever, a single LLM used in isolation is prone to inconsistencies: it ignores structural dependencies
055 among features, violates logical constraints, and cannot holistically capture the full complexity of

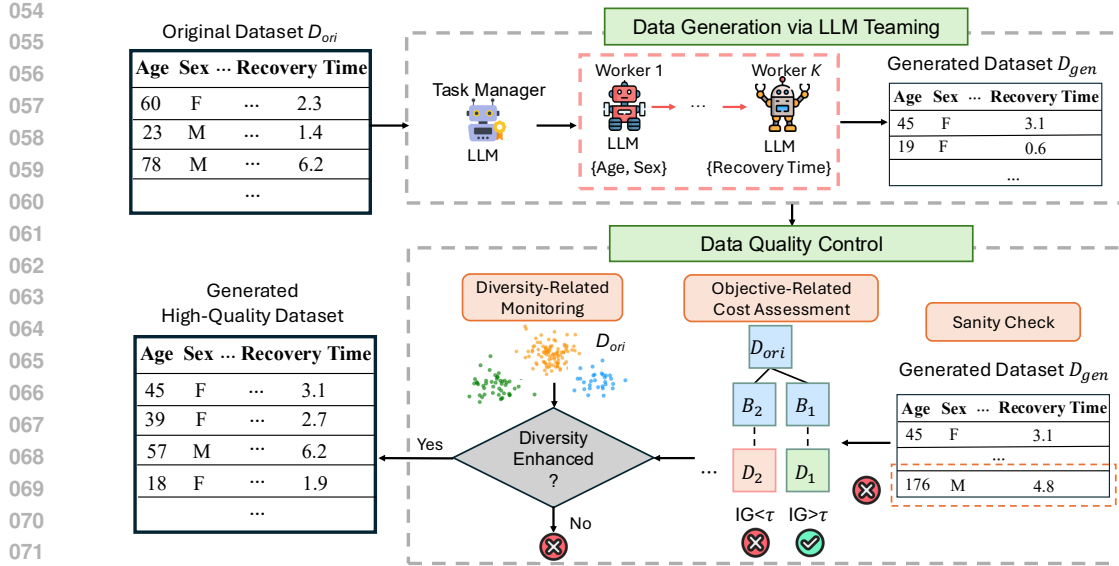


Figure 1: An illustration of our team-then-trim framework. The LLM teaming is for structured data generation and the trimming is for rigorous three-stage QC.

tabular datasets. Further related work is provided in Appendix A. These issues limit their reliability, especially when tasked with generating multi-faceted records from small seed datasets.

Beyond generation, ensuring the quality of synthetic data is equally critical. LLMs are known to hallucinate (Bang et al., 2025), introduce implausible entries (Yao et al., 2023), or produce distributions that deviate from domain requirements (Xu et al., 2024). Existing methods typically focus on plausibility checks or heuristic filtering (Sousa et al., 2024), but they often overlook deeper dimensions of quality, such as consistency with downstream objectives, fidelity to minority subgroups, and diversity of coverage. Without a principled quality control (QC) process, synthetic data risks amplifying noise rather than mitigating it.

To address these two challenges, in this paper, we introduce *team-then-trim*, a framework that combines teaming for structured data generation with trimming for rigorous three-stage QC. Unlike monolithic generators, our framework decomposes a dataset into semantically coherent components and assigns each to a specialized LLM worker with a clearly defined role. Workers operate sequentially, conditioning on previously produced components to preserve inter-feature logic and domain constraints. Team-then-trim produces data in batches, allowing large volumes of synthetic data to be created with lower cost and higher efficiency (Citovsky et al., 2021; Ren et al., 2021), while subjecting each batch to a rigorous QC process. The QC pipeline consists of three stages: (1) a sanity check validates variable ranges, categorical consistency, and inter-feature dependencies; (2) objective-related cost assessment, a model-based duel between LLM-generated batches and bootstrap samples from the original data, keeping low-residual points, and (3) diversity-related monitoring with clustering-based coverage checks that admits batches expanding coverage without skew. Together, these stages transform an initial synthetic pool into a task-aligned, diverse, and constraint-consistent dataset for downstream learning. The QC pipeline is modular and can be plugged into any generative approach. To sum up, the contributions of this paper are three-fold:

- We introduce team-then-trim, a novel framework that conceptualizes data augmentation as a product manufacturing process, where raw augmented data is initially synthesized in batches through the collaborative assembly of multiple specialized LLM generators (teaming) and subsequently refined through a rigorous QC process (trimming), ultimately yielding high-quality tabular data.
- We design a three-stage data QC pipeline to transform the raw synthetic data batches into high-quality data with only a small set of true data. The pipeline systematically refines data quality along multiple dimensions including validity, learnability, informativeness, and diversity.

- 108 • We conducted extensive experiments on various simulated and real-world datasets to demonstrate
 109 that our framework can reliably generate tabular data of high quality across diverse evaluation
 110 metrics. Its consistent superiority over state-of-the-art data augmentation methods provides strong
 111 evidence for the utility of LLMs, when coupled with effective QC, in addressing challenging ML
 112 scenarios characterized by data scarcity, imbalance, and noise, etc.

114 **2 TEAM-THEN-TRIM FRAMEWORK**

116 We now describe our team-then-trim framework for generating high-quality tabular data that can
 117 be used by a broad spectrum of downstream predictive models. Consider the tabular data space
 118 $\mathcal{X} \times \mathcal{Y}$ equipped with a probability measure induced by the true data distribution p_{true} . Here,
 119 $\mathcal{X} = \mathcal{X}_1 \times \dots \times \mathcal{X}_d$ denotes the d -dimensional feature space where \mathcal{X}_j is the j -th feature dimension,
 120 and \mathcal{Y} denotes the label space. Our framework starts with a small tabular dataset sampled from
 121 p_{true} , denoted by $D_{ori} = \{(\mathbf{x}_i, y_i)\}_{i=1}^n$, where $\mathbf{x}_i = (x_{i,1}, \dots, x_{i,d}) \in \mathcal{X}$ and $y_i \in \mathcal{Y}$. It aims
 122 to generate an additional set of new data D_{gen} without explicit knowledge of p_{true} and combine it
 123 with the original data D_{ori} to build a new dataset $D_{new} = D_{ori} \cup D_{gen}$, such that a downstream
 124 predictive model $y = f(\mathbf{x})$ trained on this augmented dataset D_{new} attains improved generaliza-
 125 tion performance compared to training exclusively on D_{ori} . An overview of the team-then-trim
 126 framework is shown in Fig. 1. We will present details in the following subsections.

127 **2.1 RAW DATA GENERATION VIA LLM TEAMING**

130 An assembly line in manufacturing typically breaks down a complex production process into a
 131 sequence of smaller subtasks which are carried out by specialized workers under the coordination of
 132 a task manager. Analogously, the team-then-trim framework employs a team of pretrained LLMs,
 133 where a task manager LLM and multiple worker LLMs collaborate to produce a raw tabular dataset.
 134 Given a data generation task, the task manager LLM, guided by its domain knowledge of the specific
 135 task and analysis of the true data D_{ori} , first decomposes the data structure into multiple components.
 136 It then assigns the subtasks of generating these components to different worker LLMs and organizes
 137 their execution according to a specified topology. The worker LLMs perform their assigned tasks to
 138 generate the components separately, following the instruction given by the task manager LLM in an
 139 assembly-line fashion.

140 **Task manager.** Given the original dataset D_{ori} , the task manager LLM Φ is additionally prompted
 141 with the feature dictionary to facilitate the understanding of the task (see Appendix Fig. 6). Based
 142 on its understanding and domain knowledge, it will partition the full feature space \mathcal{X} into K disjoint
 143 components, i.e., $\mathcal{X} = \mathcal{X}_1 \times \dots \times \mathcal{X}_{I_K}$, where $\mathcal{X}_I = \prod_{i \in I} \mathcal{X}_i$ is the cartesian product of all the single
 144 feature spaces whose indices fall in I . Thus, the partition should satisfy $\bigcup_{k=1}^K I_k = \{1, \dots, d\}$
 145 and for $\forall k, l = 1, \dots, K, k \neq l, I_k \cap I_l = \emptyset$. This partition divides the data generation work-
 146 load into K components, allowing different LLM workers to handle distinct parts of the task.
 147 Here, each component represents a coherent semantic
 148 category, with all the features share some under-
 149 lying semantical characteristics though not necessarily
 150 correlated. For example, suppose the objective is
 151 to predict the post-surgery recovery time (outcome)
 152 with four predictors: age, sex, hospital resources and
 153 sleep quality. As Fig. 2 shows, these predictors can
 154 be grouped into three categories, “age” and “sex” as
 155 demographic features, “hospital resources” as an
 156 independent environmental feature, and “sleep qual-
 157 ity” as a feature potentially influenced by both demo-
 158 graphic and environmental factors. Without incor-
 159 porating such structural knowledge, the generated data
 160 may overlook the complex dependencies among features and fail to capture their semantically mean-
 161 ingful relationships. In our team-then-trim framework, the task manager LLM fully utilizes such
 162 knowledge to coordinate the generation task. It views the different data components as nodes on a
 163 graph, which results in an activity-on-vertex network (precedence graph (Boffey, 1982)) $G = (V, E)$
 164 explicitly encoding their relationships where $V = \{I_1, \dots, I_K\}$ and E encodes the information of

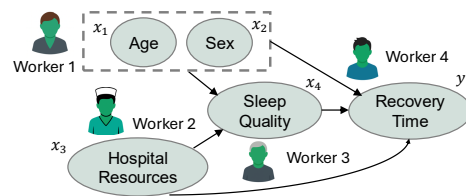


Figure 2: An example of task coordination.

162 the graph links. Thus, the work of the task manager LLM can be expressed as:
 163

$$G = \Phi(\mathcal{P}(D_{ori}, \mathbf{c})), \quad (1)$$

165 where \mathbf{c} is necessary contextual information of the dataset (e.g., variable dictionary) and \mathcal{P} denotes
 166 the encoding function that turns the input information into prompts. Through this scheduling, com-
 167 ponents without inter-dependencies can be generated in parallel, whereas those with dependency
 168 constraints should be generated sequentially. With less information required for generating each
 169 component, the overall process is enabled to produce more precise and semantically coherent data.
 170

171 **Specialized workers.** Our team-then-trim framework employs a set of LLMs Ψ_1, \dots, Ψ_K that
 172 act as specialized workers to efficiently and consistently generate the K different data components
 173 defined by the task manager LLM. All the specialized workers follow the task coordination instruc-
 174 tions provided by the task manager to generate data sequentially in the prescribed order. Each worker
 175 receives a prompt containing specific information about the component it is responsible for, along
 176 with all previously generated data components on which its assigned component may depend. The
 177 generated data component can be expressed as follows:

$$178 \quad \mathbf{X}_k \sim \Psi_k(\mathcal{P}_k(D_{ori}, \mathbf{c}_k, G) | \bigcup_{l \in \text{pa}(I_k, G)} \mathbf{X}_l), \quad \forall k = 1, \dots, K, \quad (2)$$

181 where \mathcal{P}_k is the individual prompt encoding function, $\text{pa}(I_k, G)$ denotes the set of parent nodes of
 182 I_k on graph G and \mathbf{c}_k is the contextual information about the features in the k -th component. Thus,
 183 the parent components, the generation schedule determined by the task manager and original data
 184 with contextual information together constitute the foundation for generating \mathbf{X}_k . For example, in
 185 Fig. 2, to generate the data column for the feature “sleep quality”, worker 1 and 2 should gener-
 186 ate the demographic feature component (including “age” and “sex”) and the environmental feature
 187 component (including “hospital resources”) beforehand, as it guarantees that the subsequent gener-
 188 ation of “sleep quality” does not contradict the domain knowledge encoded within the LLM worker.
 189 It is important to note that, due to the stochastic nature of LLMs, the generation process is inher-
 190 ently not deterministic. Consequently, the generated data is not fixed even with identical prompts or
 191 conditions. Once the parent components have been generated by upstream LLM workers under the
 192 coordination of the task manager, the specialized worker proceeds to sample candidate data points
 193 from an underlying, unknown distribution as instructed by the received prompt. Since the features
 194 in the same component semantically belong to the same category, each worker can focus on gener-
 195 ating semantically related concepts, which makes the generation process more efficient and reliable.
 196 Taking advantage of the prior knowledge, contextual understanding, and in-context learning capa-
 197 bilities of LLMs, the generated data is expected to exhibit higher internal consistency and factual
 198 fidelity (Saglam et al., 2025; Kozlowski et al., 2025; Wang et al., 2025) through the teaming of these
 199 workers, which is a notable advantage over a single LLM that handles multiple semantic categories
 200 simultaneously. An example that illustrates such advantage is shown in Appendix E. Finally, when
 201 all these workers finish their generation, we aggregate all the generated components and assemble
 202 them into a full design (unlabeled dataset) through a concatenation function:
 203

$$202 \quad \mathbf{X}_{gen} = \text{Concat}(\mathbf{X}_1, \dots, \mathbf{X}_K). \quad (3)$$

203 An additional LLM worker Ψ_{K+1} takes in the unlabeled dataset and generates labels for the design:
 204

$$205 \quad \mathbf{y}_{gen} \sim \Psi_{K+1}(\mathcal{P}_y(D_{ori}, \mathbf{c}, \mathbf{X})), \quad (4)$$

206 where \mathcal{P}_y is the prompt encoding function. Here, the labels can be restricted to meaningful values
 207 by encoding the constraints in the contextual information \mathbf{c} . For example, for binary labeled data,
 208 the label worker is prompted to only produce values from $\{0, 1\}$. But if not required, the worker
 209 is allowed to generate different labels beyond the ones in the given original dataset to encourage
 210 its exploration. With the labels generated, combining all together, we can end up with a complete
 211 dataset $\mathcal{D}_{gen} = \{\mathbf{X}_{gen}, \mathbf{y}_{gen}\}$.
 212

213 2.2 DATA QUALITY CONTROL

214 Given the original dataset D_{ori} with necessary contextual information, a collaborative team of LLM
 215 workers coordinated by an LLM task manager can produce a dataset in an assembly-line fashion,

similar to manufacturing production. However, even though the generated data may appear plausible, it can still suffer from quality issues due to LLM hallucination or mistakes (Huang et al., 2025; Chen et al., 2024b; Liu et al., 2024). Just as physical products require QC to ensure their reliability, the raw products of the data generation assembly line, namely, the generated data, must also undergo a quality assurance process to ensure they are readily usable by various downstream applications. Essentially, it can be extremely hard to manipulate the generation process of the LLM workers given their black-box nature. Unless we perform full training or fine-tuning with a large amount of ground-truth data to guide the LLMs, both of which typically incur substantial cost, it is difficult to exert direct control over the quality of the generated data during the generation phase. Consequently, quality assurance efforts are preferably concentrated in the post-generation stage, which motivates the design of our three-stage plug-in QC pipeline.

In our pipeline, to further refine the raw data generated by the LLM assembly line in Section 2.1, QC is performed in a batch-wise manner, trimming or discarding data as necessary. Compared to checking the quality of a single data point, the use of the batch setting has multiple advantages, such as reducing cost, improving efficiency, etc. (Citovsky et al., 2021; Ren et al., 2021). Moreover, batches inherently provide richer collective information than isolated samples, which enables more effective and informative quality inspection at the batch level (Kirsch et al., 2019). Assume the batch size is n_b . The core idea of our QC process is: each time t a small fixed-size dataset D_t is generated from the LLM assembly line as a batch, its quality is rigorously evaluated. If the batch meets the predefined quality requirements, it is polished by trimming the unsatisfied samples in the batch and integrated into the existing dataset D (initially D_{ori}) to construct a new set; otherwise, the full batch is discarded. This iterative generation-and-evaluation cycle continues until sufficient data has been admitted. For the evaluation, we ensure the batch quality from three complementary aspects: 1) Sanity check. The batch is examined on its variables to filter out apparently invalid or impossible data samples. 2) Objective-related cost assessment. Low-quality data is identified and rejected based on the batch’s total cost related to the learning objective of a specific model. 3) Diversity inspection. The batch is further checked to ensure sufficient coverage in the full data space.

Sanity check. To ensure the samples in the batch D_t is valid, we perform sanity check based on the types and values of features together with necessary relation constraints. For continuous features indexed by $S_1 = \{k_1, \dots, k_m\}$, their values in all the samples of D_t should be within a reasonable range, which can be characterized a disjunction of linear inequalities $\Omega = \Omega_1 \vee \dots \vee \Omega_m$ where Ω_i denotes a boundary inequality over the feature of the form $l_i \leq x \leq u_i$. For categorical features indexed by $S_2 = \{1, \dots, d\} \setminus S_1$, we ensure their values fall in the allowable categories C_1, \dots, C_{n_l} for any feature indexed by $l \in S_2$. By introducing dummy variables $x_{\cdot, l, 1}, \dots, x_{\cdot, l, n_l} \in \{0, 1\}$ where $x_{\cdot, l, j} = \mathbb{I}[x_{\cdot, l} \in C_j], \forall j = 1, \dots, n_l$ denotes the indicator of whether feature $x_{\cdot, l}$ belongs to a category C_j , we impose the categorical constraint $\sum_{j=1}^{n_l} x_{\cdot, l, j} = 1$. Furthermore, strict relationship among features can be expressed in a similar disjunction of inequalities of the form $\sum_{l \in S_1} w_l x_{\cdot, l} + \sum_{l \in S_2} \sum_{j=1}^{n_l} w_{l, j} x_{\cdot, l, j} + b \geq 0$ where w represents the coefficients. As a result, all requirements on feature values and their interdependence can ultimately be formulated as a unified set of logical and linear constraints. Thus, sanity check is reduced to a constraint satisfaction problem and any sample that does not satisfy the predefined constraints are discarded. In practice, thanks to the prior knowledge of LLMs, the generated batch typically satisfies these constraints most of the time. Nevertheless, this check remains indispensable for preventing trivial errors in the generated batch and eliminating semantically meaningless data that could compromise downstream tasks.

Objective-related cost assessment. Even if a data batch that passes sanity check, its utility for downstream tasks is not guaranteed, as it may still suffer from issues such as bias, imbalance, noise, etc. Since the generated data ultimately serves a predictive model, additional efforts are needed to ensure models trained on it can achieve high predictive accuracy. Thus, we focus on model-based prediction and evaluate the potential learning objective-related cost. We assume the access to the downstream model $y = f(\mathbf{x})$. To facilitate the assessment, we perform bootstrapping from the original set D_{ori} to obtain a dataset B_t of the same size as the generated batch D_t , i.e., n_b . We combine two sets as $\tilde{D}_t = D_t \bigcup B_t$ and make predictions for all the samples in \tilde{D}_t with the model f . Thus, for any sample \mathbf{x}_i in \tilde{D}_t with label y_i , we have the objective-related cost of a sample for classification tasks:

$$r_i = 1 - p_f(y_i | \mathbf{x}_i) \quad (5)$$

270 where p_f is the predicted probability score given by model f . On the one hand, to build a high-
 271 quality batch of size n_b , we aim to minimize the prediction cost. On the other hand, excessive
 272 cost minimization for the model on a small dataset may cause overfitting and potentially degrade
 273 the model’s generalization performance. Instead of pursuing either extreme, we select the 50% of
 274 the $2n_b$ samples in between to build an updated batch. We sort the costs in Eq. (5) and build an
 275 empirical distribution of the costs as F . Denote $F^{-1}(\beta) \triangleq \inf\{e : F(e) \geq \beta\}$ as the β -quantile of
 276 $\{r_i\}_{i=1}^{2n_b}$. For a specific $\beta \in (0, 0.5)$, we select the samples indexed by $J = \{i_1, \dots, i_{n_b}\}$ from \tilde{D}_t
 277 such that for $\forall i \in J$, we have

$$r_i \in [F^{-1}(\beta), F^{-1}(\beta + 0.5)] \quad (6)$$

278 These selected samples build a refined dataset $\bar{D}_t = \{(\mathbf{x}_i, y_i)\}_{i \in J}$, which can be further compared
 279 with the bootstrap set B_t . We consider the different effects of combining this refined set and the
 280 bootstrap set into the existing dataset D , which gives two sets: $D_{gen}^1 = D \cup \bar{D}_t$ and $D_{gen}^2 =$
 281 $D \cup B_t$. Following Mehta et al. (2022); Smith et al. (2023), for any dataset D' , the total information
 282 gain (IG) of combining D' with D can be calculated by

$$IG(D') = H(D \cup D') - H(D) \quad (7)$$

283 where $H(\cdot)$ is the entropy function. Thus, we can calculate the information gain of the two sets as
 284 $IG(D_{gen}^1)$ and $IG(D_{gen}^2)$, and compute their gap as $\Delta = IG(D_{gen}^1) - IG(D_{gen}^2)$, which measures
 285 the marginal information gain from the generated data batch \bar{D}_t over the original data batch \bar{B}_t . We
 286 only keep the batch of generated data when it gives us enough information, i.e., Δ is greater than a
 287 threshold τ . Thus, if $\Delta > \tau$, we merge the updated batch \bar{D}_t into the existing dataset D , otherwise
 288 we discard it.

289 **Diversity inspection.** Beyond validity and objective alignment, it is crucial to ensure that the
 290 generated data enhances (at least maintains) the diversity of D_{ori} , especially for underrepresented
 291 subpopulations. We uncover the underlying structure of D_{ori} by performing clustering. The optimal
 292 number of clusters is determined by maximizing the average silhouette score of all the data points
 293 in D_{ori} . Here, the silhouette score $s(\mathbf{x}_i)$ of a data point \mathbf{x}_i can be computed by

$$s(\mathbf{x}_i) = \frac{z^{coh}(\mathbf{x}_i) - z^{sep}(\mathbf{x}_i)}{\max\{z^{coh}(\mathbf{x}_i), z^{sep}(\mathbf{x}_i)\}} \quad (8)$$

300 where z^{coh} represents the average distance between \mathbf{x}_i and all other data points within the same
 301 cluster and z^{sep} smallest average distance between \mathbf{x}_i and all points in the nearest different cluster.
 302 After partitioning D_{ori} into these clusters, we train a multi-class classifier (i.e., an MLP) using
 303 the cluster assignments as labels. This classifier effectively learns to map any data point from the
 304 feature space to one of the identified data-space regions. If the batch of generated data D_t passes
 305 the objective-related cost assessment, we use this trained classifier to predict the cluster for each
 306 sample in the batch. To quantify the batch’s contribution to overall diversity, we measure the change
 307 in the entropy of the cluster label distribution. A batch D_t is accepted only if the percentage ent-
 308 ropy improvement of the combined dataset ($D_{ori} \cup D_t$) over the original dataset (D_{ori}) exceeds a
 309 predefined threshold. This criterion ensures that accepted batches either populate underrepresented
 310 clusters or are sufficiently varied to distribute across multiple clusters, thereby expanding coverage
 311 without introducing significant skew.

3 EXPERIMENTS AND RESULTS

312 We conduct a comprehensive evaluation of team-then-trim across both simulated studies and real-
 313 world applications. In the simulated setting, we recreate common deficiencies in tabular datasets,
 314 including imbalance, incompleteness, and noise. For data scarcity, we consider low-data regimes in
 315 experiments. For real-world datasets, we examine both the downstream utility of ML models and
 316 multiple dimensions of data quality to assess the broader impact of our framework.

3.1 SETUP

317 We employ Llama 3.3 70B Instruct as the backbone LLM for data generation. To validate that our
 318 conclusions hold across model families, we also run experiments using Grok 4.1 Fast in the data-
 319 imbalance and data-incompleteness settings. For downstream evaluation, we consider: Logistic

Regression, SVM, MLP, and Random Forest. We compare our framework, team-then-trim, against established baselines, including CLLM (Seedat et al., 2024), TVAE (Xu et al., 2019), CTGAN (Xu et al., 2019), and SMOTE (Chawla et al., 2002). For all reported results, except the baseline that uses only D_{ori} , the training data consists of the original dataset D_{ori} combined with the generated data produced by team-then-trim or by the baselines. For ablation, we include results from team-then-trim without the QC stage. In the simulated setting, we construct two datasets: (1) a diabetes prediction dataset (Rauba et al., 2024), and (2) a travel behavior dataset (Zhu et al., 2020). For real-world experiments, we adopt datasets: Drug from the UCI repository (Fehrman et al., 2017) and COMPAS from OpenML (Angwin et al., 2016). All reported results are averaged over 10 random seeds corresponding to 10 train-test splits and 4 downstream models. More experimental details are in Appendix C.

3.2 SIMULATED STUDIES

Data imbalance. In the diabetes dataset, we simulate three levels of risk groups, i.e., low risk (LR), moderate risk (MR), and high risk (HR), with a 7:2:1 ratio to create label imbalance. The size of D_{ori} is 10, following this imbalanced ratio. Table 1 reports the average AUC of different methods. Our team-then-trim framework achieves the strongest and most consistent gains across all groups. Without QC, team-then-trim already enhances AUC in HR group substantially by 12.1% over models trained on D_{ori} , highlighting the benefit of LLM-teamed generation in covering rare subpopulations. The consistently superior AUC across classes indicates that our framework with QC is particularly effective in addressing label imbalance in tabular data.

Data incompleteness. To simulate real-world incompleteness, we construct D_{ori} with LR:MR:HR = 8:2:0, such that the HR group constitutes a missing subpopulation in the training data. The size of D_{ori} is set to 10. The test set retains the distribution with LR:MR:HR = 7:2:1. Table 2 presents average AUC under this setting. Classical generation baselines completely fail to recover the missing HR subgroup. Although CLLM leverages the LLM for generation and attains relatively high AUC in the MR group, it generalizes poorly to the HR group, indicating that without explicit LLM teaming and rigorous QC, the generated samples are often noisy or misaligned. By contrast, team-then-trim demonstrates strong performance of 14.18% gain over CLLM in the HR group.

Data noise. To simulate data noise, we encode the outcome variables in both datasets as binary indicators. Larger flip ratios of the true labels correspond to higher levels of label corruption, thereby creating increasingly noisy datasets. In the diabetes dataset, at a low noise level (flip ratio = 0.2, shown in Fig. 3a), team-then-trim outperforms all models when the number of original samples is small. As the number of original samples increases, the clean data alone already yields high AUC due to the mild noise. As noise increases to 0.3 (shown in Fig. 3b) and 0.4 (shown in Fig. 3c), team-then-trim sustains stable gains. This demonstrates the framework’s robustness to label corruption

Table 1: Average AUC (%) when the label in the dataset is imbalanced.

Method	LLM Backbone	LR	MR	HR
D_{ori}	-	63.92	59.16	64.24
SMOTE	-	68.99	58.73	68.66
TVAE	-	68.79	60.75	65.22
CTGAN	-	67.30	59.61	67.00
CLLM	Grok 4.1 Fast	64.29	54.72	66.87
CLLM	Llama 3.3	64.43	57.15	65.79
Team-then-Trim (w/o QC)	Grok 4.1 Fast	65.89	56.64	75.90
Team-then-Trim	Grok 4.1 Fast	66.04	56.67	76.45
Team-then-Trim (w/o QC)	Llama 3.3	65.57	57.16	76.34
Team-then-Trim	Llama 3.3	71.55	62.03	76.98

Table 2: Average AUC (%) when the dataset is incomplete in a subpopulation.

Method	LLM Backbone	LR	MR	HR
D_{ori}	-	58.59	48.69	/
SMOTE	-	64.70	48.52	/
TVAE	-	62.81	49.85	/
CTGAN	-	65.14	49.87	/
CLLM	Grok 4.1 Fast	82.58	48.99	53.68
CLLM	Llama 3.3	63.68	54.47	50.49
Team-then-Trim (w/o QC)	Grok 4.1 Fast	82.44	51.70	56.50
Team-then-Trim	Grok 4.1 Fast	82.98	52.59	58.13
Team-then-Trim (w/o QC)	Llama 3.3	64.76	52.30	62.34
Team-then-Trim	Llama 3.3	71.16	52.26	64.67

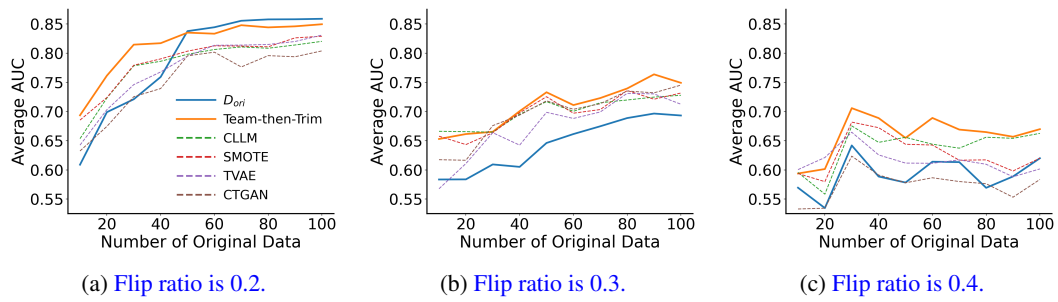


Figure 3: Average AUC across different sizes of D_{ori} under flip ratios of $\{0.2, 0.3, 0.4\}$ on Diabetes dataset.

even under moderate to severe noise. Additional performance metrics on diabetes data are presented in Appendix Table 7 and t-SNE visualizations are in Appendix Fig. 9.

Table 3 shows the average AUC under no flip, flip ratios of 0.3, and 0.4 on the TravelBehavior dataset, with 60 original samples. The observed trends mirror those in the diabetes dataset. Overall, team-then-trim enhances downstream utility across noisy settings in both datasets, with particularly strong gains under higher noise levels, highlighting its effectiveness as a generative framework for challenging real-world tabular data.

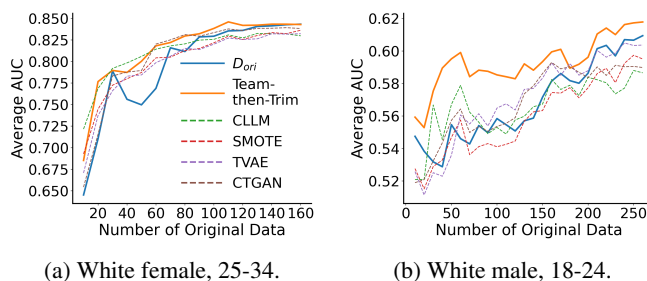


Figure 4: Average AUC for two demographic groups on Drug dataset.

Table 3: Average AUC (%) under flip ratios of $\{0, 0.3, 0.4\}$ on TravelBehavior Dataset.

Method	No Flip	0.3	0.4
D_{ori}	98.55	60.61	50.02
SMOTE	98.54	58.95	51.03
TVAE	96.62	57.80	49.11
CTGAN	91.40	58.91	49.26
CLLM	97.73	62.05	53.14
Team-then-Trim (w/o QC)	98.08	62.49	53.02
Team-then-Trim	98.24	63.44	53.38

3.3 REAL-WORLD DATA

3.3.1 DOWNSTREAM UTILITY

To assess model performance across diverse populations, we partition the Drug dataset into two subgroup datasets Drug-A and Drug-B based on their demographic features (age, gender, and ethnicity). Fig. 4a corresponds to the subgroup whose age is between 25 and 34, female, and White, while Fig. 4b focuses on White male with age between 18 and 24. Across both groups, team-then-trim outperforms baseline methods, particularly in low- and medium-data regimes. For the 18-24 male subgroup, team-then-trim delivers the highest AUC across all sample sizes from 10 to 250. The larger improvement of team-then-trim in the 18-24 male subgroup is attributed to the binary label imbalance, where 74.07% of samples are labeled as 1, compared to 63.11% in the 25-34 female subgroup. Overall, our method enhances model utility in both balanced and imbalanced settings.

Table 4: Average downstream utility (%) across different sizes of D_{ori} (10 to 200) on COMPAS dataset.

Method	Accuracy	AUC	F1	Recall
D_{ori}	60.89	64.12	58.69	60.00
SMOTE	60.77	64.86	58.43	60.20
TVAE	60.81	64.32	58.63	60.62
CTGAN	60.54	64.61	58.23	60.25
CLLM	61.70	65.54	59.26	60.90
Team-then-Trim (w/o QC)	61.32	66.82	61.46	66.87
Team-then-Trim	62.05	67.29	61.84	66.11

432
433
Table 5: Average data quality (%) across different sizes of D_{ori} on real-world data.
434

Dataset	Method	Detection	α -Precision	β -Recall
DRUG-A	SMOTE	65.71	53.97	35.50
	TVAE	65.59	53.89	35.73
	CTGAN	64.60	54.01	35.77
	CLLM	63.27	58.12	37.25
	Team-then-Trim (w/o QC)	63.00	87.38	42.62
	Team-then-Trim	56.68	88.76	48.45
DRUG-B	SMOTE	66.30	51.20	34.01
	TVAE	65.99	51.12	33.34
	CTGAN	66.15	51.23	33.25
	CLLM	63.67	56.53	35.47
	Team-then-Trim (w/o QC)	64.91	89.70	44.40
	Team-then-Trim	57.81	90.96	49.29
COMPAS	SMOTE	52.91	88.47	46.52
	TVAE	51.37	89.94	50.32
	CTGAN	51.12	91.23	51.03
	CLLM	50.26	91.58	48.63
	Team-then-Trim (w/o QC)	52.29	87.65	47.55
	Team-then-Trim	49.17	91.11	51.29

452
453
454
455
456
457
458
459
460
Table 4 provides a summary of downstream utility across varying sizes of D_{ori} on COMPAS dataset.
461 Team-then-trim achieves the best overall performance across all four metrics. Notably, the ablation
462 team-then-trim w/o QC also shows competitive improvements (e.g., recall of 66.87%), confirming
463 that LLM teaming alone provides value. Also, the full QC pipeline consistently yields higher accu-
464 racy, AUC and F1 scores, demonstrating that rigorous trimming enhances the informativeness and
465 task-alignment of generated samples. Detailed results on the average AUC of four ML models are
466 shown in Appendix Fig. 10.
467

468
469
3.3.2 DATA QUALITY

470
471
472
473
474
475
476
477
478
479
480
481
482
483
We evaluate the quality of generated data using three metrics: detection (Liu et al., 2023), α -
484 precision (Alaa et al., 2022), and β -recall (Alaa et al., 2022). Detection measures whether synthetic
485 data can be distinguished from real data, with lower scores indicating higher similarity (thus better
486 quality). α -precision quantifies the fidelity of generated samples, while β -recall captures their diver-
487 sity. [More descriptions on evaluation metrics are provided in the Appendix C](#). Table 5 shows the data
488 quality of different generation methods on the DRUG-A (subgroup in Fig. 4a), DRUG-B (subgroup
489 in Fig. 4b), and COMPAS datasets. Team-then-trim consistently outperforms baseline methods
490 except α -precision in the COMPAS dataset. This is because α -precision emphasizes high-fidelity
491 reconstruction of the densest regions of the real distribution, whereas our framework intentionally
492 trades a small amount of local fidelity for improved coverage and objective alignment. The QC
493 pipeline is designed to admit batches that increase information gain and expand cluster-level diver-
494 sity, which naturally encourages exploration beyond the tight, high-probability core modes favored
495 by α -precision. COMPAS is a dataset with well-documented fairness issues (Wang et al., 2019),
496 which means its real distribution is highly concentrated and exhibits limited feature variability. Our
497 diversity-oriented trimming can slightly pull samples away from the exact support of the majority
498 mode, yielding marginally lower α -precision. However, this trade-off is beneficial for downstream
499 learning, as reflected in consistently stronger β -recall, detection scores, and predictive performance.
500 These results demonstrate that team-then-trim generates synthetic data that are simultaneously in-
501 distinguishable from real data, faithful to the real distribution, and diverse enough to cover rare or
502 missing modes. The consistent improvements across heterogeneous datasets reinforce the effective-
503 ness of LLM teaming coupled with rigorous QC in producing high-quality tabular data.

504
505
4 CONCLUSION

506
507
508
509
510
511
512
513
In this work, we introduced team-then-trim, a novel assembly-line framework for tabular data gener-
514 ation that leverages the complementary strengths of LLMs and a principled QC pipeline. By decom-
515 posing generation into specialized LLM teams and rigorously trimming outputs through three-stage

486 checks, our approach systematically transforms raw generations into high-quality synthetic datasets.
 487 Extensive experiments across simulated deficiencies, including imbalance, incompleteness, noise
 488 and scarcity, and real-world applications demonstrate that team-then-trim consistently outperforms
 489 state-of-the-art generation methods. Notably, the framework not only improves downstream utility
 490 across diverse classifiers but also achieves superior fidelity, diversity, and indistinguishability from
 491 real data. These results highlight the potential of structured LLM teaming, coupled with rigorous
 492 data QC, to bridge critical gaps in learning scenarios with data deficiencies.

493

494 ETHICS AND REPRODUCIBILITY STATEMENT

495

496 **Ethics Statement.** This work focuses on developing a framework for generating synthetic tab-
 497 ular data to address common deficiencies such as imbalance, incompleteness, noise and scarcity
 498 in datasets. All datasets used in this paper are either simulated or publicly available datasets. No
 499 private, personally identifiable, or otherwise sensitive data were used. We adhered to responsible
 500 research practices throughout this work.

501

502 **Reproducibility Statement.** Detailed instructions for dataset access, simulation parameters, pre-
 503 processing steps and methods implementation are provided in Section 3 and Appendix C. Our code
 504 will be released publicly upon acceptance.

505

506 REFERENCES

507

508 Ahmed Alaa, Boris Van Breugel, Evgeny S Saveliev, and Mihaela Van Der Schaar. How faithful
 509 is your synthetic data? sample-level metrics for evaluating and auditing generative models. In
 510 *International conference on machine learning*, pp. 290–306. PMLR, 2022.

511

512 Carol S Aneshensel. *Theory-based data analysis for the social sciences*. Sage Publications, 2012.

513

514 Julia Angwin, Jeff Larson, Surya Mattu, and Lauren Kirchner. Machine bias url <https://www.prop->
 515 [ublica.org/article/machine-bias-risk-assessments-in-criminal-sentencing](https://www.propublica.org/article/machine-bias-risk-assessments-in-criminal-sentencing). Published on May, 23: 2016, 2016.

516

517 Yejin Bang, Ziwei Ji, Alan Schelten, Anthony Hartshorn, Tara Fowler, Cheng Zhang, Nicola
 518 Cancedda, and Pascale Fung. Hallulens: Llm hallucination benchmark. *arXiv preprint*
 519 *arXiv:2504.17550*, 2025.

520

521 Nina Baur, Peter Graeff, Lilli Braunisch, and Malte Schweia. The quality of big data. development,
 522 problems, and possibilities of use of process-generated data in the digital age. *Historical Social*
 523 *Research/Historische Sozialforschung*, 45(3):209–243, 2020.

524

525 TB Boffey. Project networks. In *Graph Theory in Operations Research*, pp. 121–147. Springer,
 526 1982.

527

528 Nitesh V Chawla, Kevin W Bowyer, Lawrence O Hall, and W Philip Kegelmeyer. Smote: synthetic
 529 minority over-sampling technique. *Journal of artificial intelligence research*, 16:321–357, 2002.

530

531 Hao Chen, Abdul Waheed, Xiang Li, Yidong Wang, Jindong Wang, Bhiksha Raj, and Marah I
 532 Abdin. On the diversity of synthetic data and its impact on training large language models. *arXiv*
 533 *preprint arXiv:2410.15226*, 2024a.

534

535 Pu Chen, Linna Wu, and Lei Wang. Ai fairness in data management and analytics: A review on
 536 challenges, methodologies and applications. *Applied sciences*, 13(18):10258, 2023.

537

538 QiHong Chen, Jiachen Yu, Jiawei Li, Jiecheng Deng, Justin Tian Jin Chen, and Iftekhar Ahmed. A
 539 deep dive into large language model code generation mistakes: What and why? *arXiv preprint*
 540 *arXiv:2411.01414*, 2024b.

541

542 Gui Citovsky, Giulia DeSalvo, Claudio Gentile, Lazaros Karydas, Anand Rajagopalan, Afshin Ros-
 543 tamizadeh, and Sanjiv Kumar. Batch active learning at scale. *Advances in Neural Information*
 544 *Processing Systems*, 34:11933–11944, 2021.

- 540 Fida K Dankar and Mahmoud Ibrahim. Fake it till you make it: Guidelines for effective synthetic
 541 data generation. *Applied Sciences*, 11(5):2158, 2021.
- 542
- 543 Elaine Fehrman, Awaz K Muhammad, Evgeny M Mirkes, Vincent Egan, and Alexander N Gorban.
 544 The five factor model of personality and evaluation of drug consumption risk. In *Data science: innovative developments in data analysis and clustering*, pp. 231–242. Springer, 2017.
- 545
- 546 Vitaly Feldman and Jan Vondrak. Generalization bounds for uniformly stable algorithms. *Advances in Neural Information Processing Systems*, 31, 2018.
- 547
- 548 Jingshuo Feng, Shuai Huang, and Cynthia Chen. Modeling user interaction with app-based re-
 549 ward system: A graphical model approach integrated with max-margin learning. *Transportation Research Part C: Emerging Technologies*, 120:102814, 2020.
- 550
- 551
- 552 Mandeep Goyal and Qusay H Mahmoud. A systematic review of synthetic data generation tech-
 553 niques using generative ai. *Electronics*, 13(17):3509, 2024.
- 554
- 555 Mandeep Goyal and Qusay H Mahmoud. An llm-based framework for synthetic data generation. In
 556 *2025 IEEE 15th Annual Computing and Communication Workshop and Conference (CCWC)*, pp.
 00340–00346. IEEE, 2025.
- 557
- 558 Shivani Gupta and Atul Gupta. Dealing with noise problem in machine learning data-sets: A sys-
 559 tematic review. *Procedia Computer Science*, 161:466–474, 2019.
- 560
- 561 Yaojie Hu, Qiang Zhou, Qihong Chen, Xiaopeng Li, Linbo Liu, Dejiao Zhang, Amit Kachroo, Talha
 562 Oz, and Omer Tripp. Qualityflow: An agentic workflow for program synthesis controlled by llm
 563 quality checks. *arXiv preprint arXiv:2501.17167*, 2025.
- 564
- 565 Lei Huang, Weijiang Yu, Weitao Ma, Weihong Zhong, Zhangyin Feng, Haotian Wang, Qianglong
 566 Chen, Weihua Peng, Xiaocheng Feng, Bing Qin, et al. A survey on hallucination in large language
 567 models: Principles, taxonomy, challenges, and open questions. *ACM Transactions on Information
 Systems*, 43(2):1–55, 2025.
- 568
- 569 Zaid Khan, Elias Stengel-Eskin, Jaemin Cho, and Mohit Bansal. Dataenvgym: Data generation
 570 agents in teacher environments with student feedback. *arXiv preprint arXiv:2410.06215*, 2024.
- 571
- 572 Andreas Kirsch, Joost Van Amersfoort, and Yarin Gal. Batchbald: Efficient and diverse batch
 573 acquisition for deep bayesian active learning. *Advances in neural information processing systems*,
 32, 2019.
- 574
- 575 Austin C Kozlowski, Callin Dai, and Andrei Bouteilne. Semantic structure in large language model
 576 embeddings. *arXiv preprint arXiv:2508.10003*, 2025.
- 577
- 578 Yi Li and Nuno Vasconcelos. Repair: Removing representation bias by dataset resampling. In
 579 *Proceedings of the IEEE/CVF conference on computer vision and pattern recognition*, pp. 9572–
 9581, 2019.
- 580
- 581 Yisen Li, Lingfeng Yang, Wenzuan Shen, Pan Zhou, Yao Wan, Weiwei Lin, and Dongping
 582 Chen. Crowdselect: Synthetic instruction data selection with multi-llm wisdom. *arXiv preprint
 arXiv:2503.01836*, 2025.
- 583
- 584 Feng Lin, Xiaoning Qian, Bobak Mortazavi, Zhangyang Wang, Shuai Huang, and Cynthia Chen.
 585 Modeling user choice behavior under data corruption: Robust learning of the latent decision
 threshold model. *IISE Transactions*, 56(12):1307–1320, 2024.
- 586
- 587 Roderick JA Little and Donald B Rubin. *Statistical analysis with missing data*. John Wiley & Sons,
 2019.
- 588
- 589 Fang Liu, Yang Liu, Lin Shi, Houkun Huang, Ruifeng Wang, Zhen Yang, Li Zhang, Zhongqi Li,
 590 and Yuchi Ma. Exploring and evaluating hallucinations in llm-powered code generation. *arXiv
 preprint arXiv:2404.00971*, 2024.
- 591
- 592 Tennison Liu, Zhaozhi Qian, Jeroen Berrevoets, and Mihaela van der Schaar. Goggle: Generative
 593 modelling for tabular data by learning relational structure. In *The Eleventh International Conference
 on Learning Representations*, 2023.

- 594 Yunbo Long, Liming Xu, and Alexandra Brintrup. Llm-tabflow: Synthetic tabular data generation
 595 with inter-column logical relationship preservation. *arXiv preprint arXiv:2503.02161*, 2025.
 596
- 597 Raghav Mehta, Changjian Shui, Brennan Nichyporuk, and Tal Arbel. Information gain sampling
 598 for active learning in medical image classification. In *International Workshop on Uncertainty for*
 599 *Safe Utilization of Machine Learning in Medical Imaging*, pp. 135–145. Springer, 2022.
- 600 Ajay Patel, Colin Raffel, and Chris Callison-Burch. Datadreamer: A tool for synthetic data genera-
 601 tion and reproducible llm workflows. *arXiv preprint arXiv:2402.10379*, 2024.
- 602
- 603 F. Pedregosa, G. Varoquaux, A. Gramfort, V. Michel, B. Thirion, O. Grisel, M. Blondel, P. Pretten-
 604 hofer, R. Weiss, V. Dubourg, J. Vanderplas, A. Passos, D. Cournapeau, M. Brucher, M. Perrot, and
 605 E. Duchesnay. Scikit-learn: Machine learning in Python. *Journal of Machine Learning Research*,
 606 12:2825–2830, 2011.
- 607 Lloyd P Provost and Sandra K Murray. *The health care data guide: learning from data for improve-
 608 ment*. John Wiley & Sons, 2022.
- 609 Zhaozhi Qian, Bogdan-Constantin Cebere, and Mihaela van der Schaar. Synthcity: facilitating inno-
 610 vative use cases of synthetic data in different data modalities. *arXiv preprint arXiv:2301.07573*,
 611 2023.
- 612
- 613 Paulius Rauba, Nabeel Seedat, Krzysztof Kacprzyk, and Mihaela van der Schaar. Self-healing ma-
 614 chine learning: A framework for autonomous adaptation in real-world environments. *Advances*
 615 *in Neural Information Processing Systems*, 37:42225–42267, 2024.
- 616 Pengzhen Ren, Yun Xiao, Xiaojun Chang, Po-Yao Huang, Zihui Li, Brij B Gupta, Xiaojiang Chen,
 617 and Xin Wang. A survey of deep active learning. *ACM computing surveys (CSUR)*, 54(9):1–40,
 618 2021.
- 619
- 620 Baturay Saglam, Paul Kassianik, Blaine Nelson, Sajana Weerawardhena, Yaron Singer, and Amin
 621 Karbasi. Large language models encode semantics in low-dimensional linear subspaces. *arXiv*
 622 *preprint arXiv:2507.09709*, 2025.
- 623 Sebastian Schelter, Dustin Lange, Philipp Schmidt, Meltem Celikel, Felix Biessmann, and Andreas
 624 Grafberger. Automating large-scale data quality verification. *Proceedings of the VLDB Endow-
 625 ment*, 11(12):1781–1794, 2018.
- 626
- 627 Sebastian Schelter, Stefan Grafberger, Philipp Schmidt, Tammo Rukat, Mario Kiessling, Andrey
 628 Taptunov, Felix Biessmann, and Dustin Lange. Differential data quality verification on partitioned
 629 data. In *2019 IEEE 35th International Conference on Data Engineering (ICDE)*, pp. 1940–1945.
 630 IEEE, 2019.
- 631
- 632 Nabeel Seedat, Nicolas Huynh, Boris van Breugel, and Mihaela van der Schaar. Curated llm: Sy-
 633 ergy of llms and data curation for tabular augmentation in ultra low-data regimes. 2023.
- 634
- 635 Nabeel Seedat, Nicolas Huynh, Boris Van Breugel, and Mihaela Van Der Schaar. Curated llm:
 636 Synergy of llms and data curation for tabular augmentation in low-data regimes. In *International
 637 Conference on Machine Learning*, pp. 44060–44092. PMLR, 2024.
- 638
- 639 Junrong Shi, Minkai Xu, Harper Hua, Hengrui Zhang, Stefano Ermon, and Jure Leskovec. Tabdiff:
 640 a mixed-type diffusion model for tabular data generation. *arXiv preprint arXiv:2410.20626*, 2024.
- 641
- 642 Luísa Shimabucoro, Sebastian Ruder, Julia Kreutzer, Marzieh Fadaee, and Sara Hooker. Llm
 643 see, llm do: Guiding data generation to target non-differentiable objectives. *arXiv preprint*
 644 *arXiv:2407.01490*, 2024.
- 645
- 646 Freddie Bickford Smith, Andreas Kirsch, Sebastian Farquhar, Yarin Gal, Adam Foster, and Tom
 647 Rainforth. Prediction-oriented bayesian active learning. In *International conference on artificial
 648 intelligence and statistics*, pp. 7331–7348. PMLR, 2023.
- 649
- 650 Jose Leandro Sousa, Cristian Souza, Raiza Hanada, Diogo Nascimento, and Eliane Collins. Genera-
 651 tion of test datasets using llm-quality assurance perspective. In *Simpósio Brasileiro de Engenharia
 652 de Software (SBES)*, pp. 644–650. SBC, 2024.

- 648 Heidi Carolina Tamm and Anastasija Nikiforova. From data quality for ai to ai for data quality:
 649 A systematic review of tools for ai-augmented data quality management in data warehouses. In
 650 *Perspectives in Business Informatics Research: 24th International Conference, BIR 2025, Riga,*
 651 *Latvia, September 17–19, 2025, Proceedings*, pp. 37. Springer Nature, 2025.
- 652 Ruixiang Tang, Xiaotian Han, Xiaoqian Jiang, and Xia Hu. Does synthetic data generation of llms
 653 help clinical text mining? *arXiv preprint arXiv:2303.04360*, 2023.
- 654 Fadi Thabtah, Suhel Hammoud, Firuz Kamalov, and Amanda Gonsalves. Data imbalance in classi-
 655 fication: Experimental evaluation. *Information Sciences*, 513:429–441, 2020.
- 656 Chenyu Wang, Weichao Zhou, Shantanu Ghosh, Kayhan Batmanghelich, and Wenchao Li. Semantic
 657 consistency-based uncertainty quantification for factuality in radiology report generation. In
 658 *NAACL (Findings)*, 2025.
- 659 Hanchen Wang, Nina Grgic-Hlaca, Preethi Lahoti, Krishna P Gummadi, and Adrian Weller. An
 660 empirical study on learning fairness metrics for compas data with human supervision. *arXiv*
 661 *preprint arXiv:1910.10255*, 2019.
- 662 Hao Wang, Shivchander Sudalairaj, John Henning, Kristjan Greenewald, and Akash Srivastava.
 663 Post-processing private synthetic data for improving utility on selected measures. *Advances in*
 664 *Neural Information Processing Systems*, 36:64139–64154, 2023.
- 665 Simon Washington, Matthew G Karlaftis, Fred Mannering, and Panagiotis Anastasopoulos. *Statis-
 666 tical and econometric methods for transportation data analysis*. Chapman and Hall/CRC, 2020.
- 667 Lei Xu, Maria Skoularidou, Alfredo Cuesta-Infante, and Kalyan Veeramachaneni. Modeling tabular
 668 data using conditional gan. *Advances in neural information processing systems*, 32, 2019.
- 669 Ziwei Xu, Sanjay Jain, and Mohan Kankanhalli. Hallucination is inevitable: An innate limitation of
 670 large language models. *arXiv preprint arXiv:2401.11817*, 2024.
- 671 Dayu Yang, Natawut Monaikul, Amanda Ding, Bozhao Tan, Kishore Mosaliganti, and Giri Iyen-
 672 gar. Enhancing table representations with llm-powered synthetic data generation. *arXiv preprint*
 673 *arXiv:2411.03356*, 2024.
- 674 Jia-Yu Yao, Kun-Peng Ning, Zhen-Hui Liu, Mu-Nan Ning, Yu-Yang Liu, and Li Yuan. Llm
 675 lies: Hallucinations are not bugs, but features as adversarial examples. *arXiv preprint*
 676 *arXiv:2310.01469*, 2023.
- 677 Xi Zhu, Feilong Wang, Cynthia Chen, and Derek D Reed. Personalized incentives for promoting
 678 sustainable travel behaviors. *Transportation Research Part C: Emerging Technologies*, 113:314–
 679 331, 2020.
- 680
- 681
- 682
- 683
- 684
- 685
- 686
- 687
- 688
- 689
- 690
- 691
- 692
- 693
- 694
- 695
- 696
- 697
- 698
- 699
- 700
- 701

702 A RELATED WORK
703
704

705 **Tabular Data Generation.** Synthetic tabular data generation has evolved from statistical methods
706 to deep generative models (Chawla et al., 2002; Xu et al., 2019; Goyal & Mahmoud, 2024; Dankar
707 & Ibrahim, 2021). GOGGLE (Liu et al., 2023) learns an explicit relational structure among columns
708 and jointly trains a message-passing VAE, enabling better modeling of sparse, heterogeneous de-
709 pendencies in tabular data. TabDiff (Shi et al., 2024) proposes a unified mixed-type diffusion model
710 that jointly handles numerical and categorical columns in continuous time, with feature-wise learn-
711 able noise schedules and a transformer denoiser. LLMs represent a paradigm shift, leveraging vast
712 pre-trained knowledge to generate data for scenarios absent in the original dataset (Tang et al., 2023;
713 Patel et al., 2024; Shimabucoro et al., 2024). CLLM (Seedat et al., 2024) leverages a frozen LLM
714 to generate tabular samples in ultra-low-data settings and then curates them via learning-dynamics
715 signals. DataEnvGym (Khan et al., 2024) introduces a modular teacher-student testbed where data
716 generation agents plan and synthesize training data in a feedback loop to improve a student model,
717 framing generation as sequential decision-making. Goyal & Mahmoud (2025) present a practical
718 platform that fine-tunes LLMs and integrates differential privacy to generate datasets while pre-
719 serving sensitive information. Yang et al. (2024) define table similarity via realistic analyst-style
720 transformations and introduces an LLM-driven pipeline that generates large-scale pairs of similar
721 tables to train and evaluate table-level embeddings. However, single LLM can hallucinate unseen
722 categories, violate hard constraints and struggle to capture complex conditional distributions. Our
723 framework, team-then-trim, addresses these gaps by decomposing generation into a manufac-
724 turing assembly line and integrating a rigorous three-stage QC pipeline to ensure the final dataset is
725 plausible and task-aligned.

726 **Data Quality Control.** QC for synthetic data has matured from ad-hoc checks to systematic, scal-
727 able pipelines that validate schemas and repair errors (Baur et al., 2020; Tamm & Nikiforova, 2025;
728 Alaa et al., 2022). Schelter et al. (2018) supports incremental metric computation on growing
729 datasets, and adds ML-assisted predictability and anomaly detection to automate large-scale data
730 quality verification. Building on this work, Schelter et al. (2019) propose a differential extension
731 that represents data-quality metrics as algebraic states with commutative-monoid properties, en-
732 abling incremental, partition-aware verification without rescanning previously processed data. Re-
733 cent advances increasingly emphasize QC for LLM-generated data (Chen et al., 2024a; Hu et al.,
734 2025). Sousa et al. (2024) apply a human protocol to deduplicate, filter out-of-scope samples before
735 using the curated set from LLMs and underscore the need for human validation. Wang et al. (2023)
736 introduce a model-agnostic, differential privacy-preserving post-processing method that reweights
737 a synthetic dataset via information projection so that selected utility measures, e.g., moments, cor-
738 relations, match noisy targets from the real data. LLM-TabLogic (Long et al., 2025) uses LLM
739 prompting to infer and compress inter-column logical relationships and then conditions a latent
740 diffusion generator on these constraints, producing synthetic tables that better preserve logical con-
741 sistency while maintaining strong fidelity and privacy. CROWDSELECT (Li et al., 2025) aggregates
742 multiple LLMs' responses and reward scores to compute three metrics with diversity clustering and
743 multi-metric normalization to select synthetic instruction data. However, these methods remain
744 pointwise and model-agnostic, and do not guarantee that admitted samples are useful for the down-
745 stream task or that they cover rare modes. Our framework, team-then-trim, addresses these gaps
746 by coupling a manufacturing-style assembly line with a three-stage QC that is explicitly task-linked
747 and batch-level.

748
749 B PROMPT EXAMPLES
750
751

752 We provide prompt examples of the LLM task manager in Fig. 6, along with one of its assigned
753 roles, the LLM Demographic and Lifestyle Synthesizer, in Fig. 7, and a subsequent role, the LLM
754 Glucose Regulation Simulator, in Fig. 8. In the prompts, we provide detailed task instructions along
755 with the definitions of all features to help LLMs clearly understand the assignment and generation
tasks.

756	Age	Physical Activity	BMI	Blood Pressure	Cholesterol	HbA1c	Fasting Glucose	Insulin	y
757	32	2	24	109	222	5.26	104	8	1
758	38	2	30	94	129	5.5	85	27	2
759	56	5	20	127	153	4.87	115	15	1
760	44	4	16	93	163	5.15	130	94	3
761	...								
762									
763									
764	Figure 5: Examples of original data in Diabetes dataset.								
765									
766									
767	C EXPERIMENTAL DETAILS								
768									
769									
770	Datasets simulation. In the simulated studies, the features of the Diabetes dataset and their co- efficients are generated following the distributions in Rauba et al. (2024), with label probabilities computed using the sigmoid function. Figure 5 shows examples of original data in the simulated Diabetes. The dataset includes eight features and one outcome label y . For the TravelBehavior dataset, features are simulated according to the distributions in Feng et al. (2020); Lin et al. (2024), and ground-truth labels are assigned using their proposed Latent Decision Threshold model. The simulated TravelBehavior dataset consists of four features and one binary outcome label. In both datasets, we construct a test set of 500 samples, while the size of the original training data varies from 10 to 100, increasing in steps of 10. Unless otherwise specified, the data generation adheres to the aforementioned distributions. We use symmetric label flipping in all noise experiments. Specif- ically, for a given flip ratio, we uniformly sample a subset of data points without conditioning on class and randomly flip their labels. Thus, every class is equally likely to be corrupted, and no class receives preferential or targeted noise.								
771									
772									
773									
774									
775									
776									
777									
778									
779									
780									
781									
782									
783	Real-world datasets. For the real-world applications, the Drug dataset from the UCI repository (Fehrman et al., 2017) is partitioned by age, gender, and ethnicity, and we only retain subgroups with more than 250 observations to ensure sufficient training and test data. After partition, the dataset consists of 24 features and one binary label outcome. For each subgroup, 100 samples are held out as the test set, with the remainder used for training after stratifying by label distribution. In the COMPAS dataset from OpenML (Angwin et al., 2016), the number of training data varies across experiments with balanced labels, and 500 samples are reserved for testing. The COMPAS dataset consists of 13 features and one binary label outcome.								
784									
785									
786									
787									
788									
789									
790									
791									
792	Data generation. Considering plausibility of evaluation and the token limits, we generate 10 data points in each batch for Diabetes and Drug datasets, and 20 data points in each batch for the Travel- Behavior and COMPAS datasets. In the data imbalance and incompleteness experiments, the number of generated batches before trimming is fixed at 10. In all other experiments with varying original data, it is set equal to the size of the original dataset; for example, with 10 original samples, one batch is generated. No additional batches are added after trimming. This design ensures that the amount of synthetic data scales proportionally with the available data, preventing over-generation.								
793									
794									
795									
796									
797									
798									
799									
800	QC. In step 2 objective-related cost assessment of QC pipeline, to calculate the threshold, we run 1000 times to obtain the mean and standard deviation. The coefficient of standard deviation ranging from 0 to 3 is selected by 5-fold cross validation. In step 3 diversity-related monitoring, we choose the number of clusters from $\{3, 4, 5\}$ to maximize the silhouette scores. The entropy improvement threshold is set as 30%.								
801									
802									
803									
804									
805									
806	Models. All the downstream models are implemented by scikit-learn (Pedregosa et al., 2011). All the experiments are run on Apple M3 Pro. We use SynthCity (Qian et al., 2023) to implement the baseline methods and to evaluate the α -precision and β -recall, except for CLLM, which follows the implementation details in Seedat et al. (2024). The detection score is computed following the procedure in Liu et al. (2023).								
807									
808									
809									
756	Age	Physical Activity	BMI	Blood Pressure	Cholesterol	HbA1c	Fasting Glucose	Insulin	y
757	32	2	24	109	222	5.26	104	8	1
758	38	2	30	94	129	5.5	85	27	2
759	56	5	20	127	153	4.87	115	15	1
760	44	4	16	93	163	5.15	130	94	3
761	...								
762									
763									
764	Figure 5: Examples of original data in Diabetes dataset.								
765									
766									
767	C EXPERIMENTAL DETAILS								
768									
769									
770	Datasets simulation. In the simulated studies, the features of the Diabetes dataset and their co- efficients are generated following the distributions in Rauba et al. (2024), with label probabilities computed using the sigmoid function. Figure 5 shows examples of original data in the simulated Diabetes. The dataset includes eight features and one outcome label y . For the TravelBehavior dataset, features are simulated according to the distributions in Feng et al. (2020); Lin et al. (2024), and ground-truth labels are assigned using their proposed Latent Decision Threshold model. The simulated TravelBehavior dataset consists of four features and one binary outcome label. In both datasets, we construct a test set of 500 samples, while the size of the original training data varies from 10 to 100, increasing in steps of 10. Unless otherwise specified, the data generation adheres to the aforementioned distributions. We use symmetric label flipping in all noise experiments. Specif- ically, for a given flip ratio, we uniformly sample a subset of data points without conditioning on class and randomly flip their labels. Thus, every class is equally likely to be corrupted, and no class receives preferential or targeted noise.								
771									
772									
773									
774									
775									
776									
777									
778									
779									
780									
781									
782									
783	Real-world datasets. For the real-world applications, the Drug dataset from the UCI repository (Fehrman et al., 2017) is partitioned by age, gender, and ethnicity, and we only retain subgroups with more than 250 observations to ensure sufficient training and test data. After partition, the dataset consists of 24 features and one binary label outcome. For each subgroup, 100 samples are held out as the test set, with the remainder used for training after stratifying by label distribution. In the COMPAS dataset from OpenML (Angwin et al., 2016), the number of training data varies across experiments with balanced labels, and 500 samples are reserved for testing. The COMPAS dataset consists of 13 features and one binary label outcome.								
784									
785									
786									
787									
788									
789									
790									
791									
792	Data generation. Considering plausibility of evaluation and the token limits, we generate 10 data points in each batch for Diabetes and Drug datasets, and 20 data points in each batch for the Travel- Behavior and COMPAS datasets. In the data imbalance and incompleteness experiments, the number of generated batches before trimming is fixed at 10. In all other experiments with varying original data, it is set equal to the size of the original dataset; for example, with 10 original samples, one batch is generated. No additional batches are added after trimming. This design ensures that the amount of synthetic data scales proportionally with the available data, preventing over-generation.								
793									
794									
795									
796									
797									
798									
799									
800	QC. In step 2 objective-related cost assessment of QC pipeline, to calculate the threshold, we run 1000 times to obtain the mean and standard deviation. The coefficient of standard deviation ranging from 0 to 3 is selected by 5-fold cross validation. In step 3 diversity-related monitoring, we choose the number of clusters from $\{3, 4, 5\}$ to maximize the silhouette scores. The entropy improvement threshold is set as 30%.								
801									
802									
803									
804									
805									
806	Models. All the downstream models are implemented by scikit-learn (Pedregosa et al., 2011). All the experiments are run on Apple M3 Pro. We use SynthCity (Qian et al., 2023) to implement the baseline methods and to evaluate the α -precision and β -recall, except for CLLM,								

810
811
812
813
814
815
816
817
818
819
820
821
822

Prompt Example for LLM Task Manager

823
824 You are a Task Manager in a diabetes research system, overseeing the assignment of roles to various Large
825 Language Models (LLMs). Each LLM is to be assigned a specific role, such as "Alternative Designer" or "Simulated
826 User," to augment distinct aspects of dataset concerning individual health condition. The dataset includes
827 individual features with their meanings provided and the outcome label is y, the diabetes indicator .

828 **Task:** Assign appropriate roles to LLMs and organize them into a sequence that facilitates collaborative
829 augmentation of the dataset. This sequence should reflect the logical relationships and dependencies between the
830 roles to maximize the efficiency and effectiveness of data augmentation.

831 **Features and Their Meanings:**

832 HbA1c: Hemoglobin A1c levels
833 FastingGlucose: Fasting glucose levels
834 Age: Age
835 BMI: Body Mass Index
836 BloodPressure: Blood pressure
837 Cholesterol: Cholesterol levels
838 Insulin: Insulin levels
839 PhysicalActivity: Physical activity levels
y: Diabetes indicator (0 = No diabetes, 1 = Diabetes)

840 **Output Requirements:** Generate a structured JSON detailing the role assignments and the sequence of
841 augmentation. You are encouraged to create new roles or modify existing ones as necessary. Ensure that each
842 feature is managed by one specific role. Also, organize the roles in a sequence ("Relationship") where the output of
843 one role feeds into the next, facilitating seamless data augmentation. Here is the required JSON structure:

844 {"Roles":
845 {"Role1": {"Name": "Role name", "Features": "Features it needs to augment"},
846 "Role2": {"Name": "Role name", "Features": "Features it needs to augment"},
847 "Role3": {"Name": "Role name", "Features": "Features it needs to augment"},
848 "Role4": {"Name": "Role name", "Features": "Features it needs to augment"},
849 "Relationship":
850 {"Order 1": "Which LLM should first augment features?",
851 "Order 2": "Which LLM should secondly augment features?",
852 "Order 3": "Which LLM should thirdly augment features?",
853 "Order 4": "Which LLM should lastly augment features?"}}.

854
855
856
857
858
859
860
861
862
863

Figure 6: Prompt example of task manager LLM.

864

865

866

867

868

869

870

871

872

873

874

875

876

877

878

879

880

881

882

883

884

885

886

887

888

889

890

891

892

893

894

895

896

897

898

899

900

901

902

Prompt Example for LLM Demographic and Lifestyle Synthesizer

You are a Demographic and Lifestyle Synthesizer in diabetes research system. Your task is to thoughtfully and realistically generate 10 novel individuals. Please think step by step and incorporate patterns learned from real-world users. You need to generate diverse and plausible combinations of the following features: "Age", and "PhysicalActivity". You are provided with 10 representative examples of real users, which include both these features and additional ones known to be associated with decision making. Use these examples to infer realistic feature relationships, but do not copy them directly.

Features and Their Meanings:

Age: Age

PhysicalActivity: Physical activity levels

BMI: Body Mass Index

BloodPressure: systolic blood pressure

Cholesterol: Cholesterol levels

HbA1c: Hemoglobin A1c levels

FastingGlucose: Fasting glucose levels

Insulin: Insulin levels

y: Diabetes indicator (0 = No diabetes, 1 = Diabetes)

Example data:

{example_data_text}

Output Requirements: The output should be a markdown code snippet formatted in the following schema, including the leading and trailing "json" and "```":

```
```json
{
 "Age": string,
 "PhysicalActivity": string,
}
}
```

Figure 7: Prompt example of an assigned role by the LLM, i.e., demographic and lifestyle synthesizer.

**Evaluation metrics.** We use various evaluation metrics to capture different aspects of downstream predictive performance and quality of generated data. AUC measures the probability that a randomly chosen positive sample receives a higher predicted score than a randomly chosen negative sample. AUC is threshold-independent and particularly informative in imbalanced settings, which is why it serves as one of our primary metrics. Accuracy provides a holistic overview of performance but may be less informative under label imbalance. Recall measures the fraction of positive samples that are correctly identified. F1-score balances the trade-off between precision and recall and serves as a compact summary of classifier performance when neither error mode is dominant.

## D ADDITIONAL RESULTS

**LLM workers.** Task manager LLM assigns different roles for different datasets. For diabetes dataset, the LLM roles are Demographic and Lifestyle Synthesizer, Glucose Regulation Simulator, Cardiometabolic Generator, and Diabetes Expert. For TravelBehavior dataset, the LLM roles are Alternative Designer, Incentive Allocator, and Decision Predictor. For Drug dataset, the LLM roles are Demographic Profiler, Personality Synthesizer, Drug Usage Generator, and Nicotine Propensity Estimator. For COMPAS dataset, the LLM roles are Demographic Profile Designer, Juvenile History Synthesizer, Criminal Record Analyst and Recidivism Outcome Evaluator.

**Data incompleteness.** We visualize the t-SNE embeddings of the MR and HR groups in Fig. 9 given the training set missing the HR subgroup on diabetes data. In both groups, the team-then-trim samples closely intermingle with the test samples, indicating that the generated data preserves the manifold structure of the real-world distribution. This alignment reflects the ability of our LLM-teamed generation, followed by QC, to enrich existing but underrepresented or even missing subpopulations with high fidelity. The results show that, unlike classical baselines, team-then-trim can generalize beyond observed data to reconstruct missing modes in the distribution. This capability enables downstream models to achieve strong performance on previously unseen subgroups.

918  
919  
920  
921  
922  
923  
924  
925  
926

**Prompt Example for LLM Glucose Regulation Simulator**  
You are a Glucose Regulation Simulator in a diabetes research system. Your task is to thoughtfully and realistically generate 10 novel individuals given their features Age and PhysicalActivity. Please think step by step and incorporate patterns learned from real-world users. You need to generate diverse and plausible combinations of the following features: "HbA1c", "FastingGlucose", and "Insulin". You are provided with 10 representative examples of real users, which include both these features and additional ones known to be associated with decision making. Use these examples to infer realistic feature relationships, but do not copy them directly

**Features and Their Meanings:**

Age: Age  
PhysicalActivity: Physical activity levels  
BMI: Body Mass Index  
BloodPressure: systolic blood pressure  
Cholesterol: Cholesterol levels  
HbA1c: Hemoglobin A1c levels  
FastingGlucose: Fasting glucose levels  
Insulin: Insulin levels  
y: Diabetes indicator (0 = No diabetes, 1 = Diabetes)

**Example data:**

{example\_data\_text}

**Output Requirements:** The output should be a markdown code snippet formatted in the following schema, including the leading and trailing "json" and "```":

```
```json
{
  {"Age": 23,
  "PhysicalActivity": 4,
  "HbA1c": string,
  "FastingGlucose": string,
  "Insulin": string.
  },
  {"Age": 47,
  "PhysicalActivity": 2,
  "HbA1c": string,
  "FastingGlucose": string,
  "Insulin": string.
  },
  ...
}
```

953
954
955
956
957
958
959
960
961
962
963
964
965
966
967
968
969
970
971

Figure 8: Prompt example of an assigned role by the LLM, i.e., glucose regulation simulator, following LLM demographic and lifestyle synthesizer.

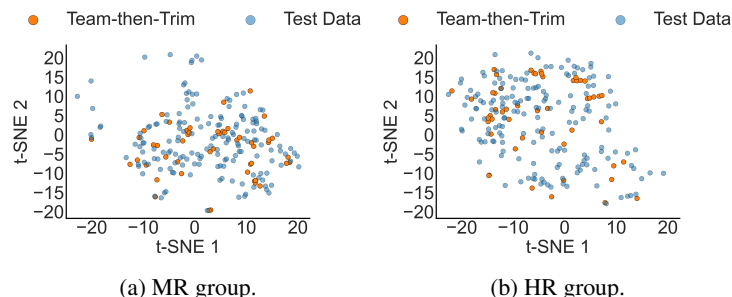


Figure 9: t-SNE plots of MR and HR groups when the dataset is incomplete.

972 Table 6: Average AUC (%) with 95% CI when the label in the dataset is imbalanced on simulated
 973 Diabetes dataset.

975 Methods	976 LR	977 MR	978 HR
977 D_{ori}	978 0.64 ± 0.15	979 0.59 ± 0.14	980 0.64 ± 0.04
980 CLLM	981 0.64 ± 0.12	982 0.57 ± 0.10	983 0.66 ± 0.16
983 Team-then-Trim (w/o QC)	984 0.66 ± 0.11	985 0.57 ± 0.09	986 0.76 ± 0.09
986 Team-then-Trim (after QC Step 1)	987 0.66 ± 0.11	988 0.57 ± 0.09	989 0.76 ± 0.09
989 Team-then-Trim (after QC Step 2)	990 0.68 ± 0.14	991 0.59 ± 0.12	992 0.76 ± 0.10
992 Team-then-Trim	993 0.72 ± 0.19	994 0.62 ± 0.17	995 0.77 ± 0.11

985 **Analysis of QC steps.** Table 6 shows that each QC stage incrementally improves AUC under the
 986 data-imbalance setting of simulated Diabetes dataset. The LLM teaming output (w/o QC) already
 987 enhances HR performance by expanding coverage of rare cases, but offers limited gains for LR and
 988 MR due to noisy or misaligned samples. Sanity check (Step 1) yields no change, consistent with the
 989 fact that LLM teaming rarely violates basic constraints. Objective-related cost assessment (Step 2)
 990 produces the first clear improvement by removing samples with poor predictive alignment, which
 991 increases AUC in both LR and MR. Diversity-related monitoring (Step 3) delivers the final boost
 992 by admitting only batches that enhance cluster-level coverage. Together, the three stages refine raw
 993 generations into data that is simultaneously valid, task-aligned, and diverse, yielding the highest
 994 AUC across all groups. The confidence intervals (CIs) become slightly wider after QC because
 995 the trimming process reduces the number of retained samples and increases the variability across
 996 random seeds.

997 **Data noise.** Table 7 reports the average performance on the diabetes dataset under varying levels
 998 of label noise, with flip ratios of 0.2, 0.3, and 0.4. Under moderate and high label corruption, both
 1000 team-then-trim and its ablation without QC sustain strong performance across the metrics, delivering
 1001 the most consistent improvements. The gains over D_{ori} and all baselines highlight the effectiveness
 1002 of combining LLM teaming with rigorous trimming in filtering out mislabeled or uninformative
 1003 samples. At a low noise level (flip ratio = 0.2), all methods achieve relatively high AUC, F1 scores
 1004 and recall, reflecting the mild corruption. Team-then-trim achieves the best AUC of 81.42% and
 1005 competitive F1 and recall. This indicates that even when data are only lightly corrupted, our frame-
 1006 work provides additional robustness without overfitting to mislabeled samples.

1007 **Computational costs of LLM-based data generation.** To contextualize the computational costs
 1008 of our framework, we examine the token usage and runtime of each LLM component during data
 1009 generation under the diabetes data-imbalance setting. Because the QC stage relies on lightweight
 1010 procedures and small models relative to our data size, its computational overhead is negligible com-
 1011 pared with the cost of LLM-based generation. The final generated dataset has a dimensionality of
 1012 10 rows \times 9 columns. As shown in Table 8, team-then-trim incurs moderately higher token con-
 1013 sumption and runtime than CLLM; however, the framework remains cost-efficient given its substan-
 1014 tially stronger downstream utility. Specifically, Table 1 shows that team-then-trim improves AUC
 1015 by 7.12% in the LR group, 4.88% in the MR group, and 11.19% in the HR group compared with
 1016 CLLM. These gains highlight that structured LLM teaming does not introduce prohibitive overhead
 1017 and, in fact, achieves a highly favorable cost–benefit tradeoff in data-deficiency regimes.

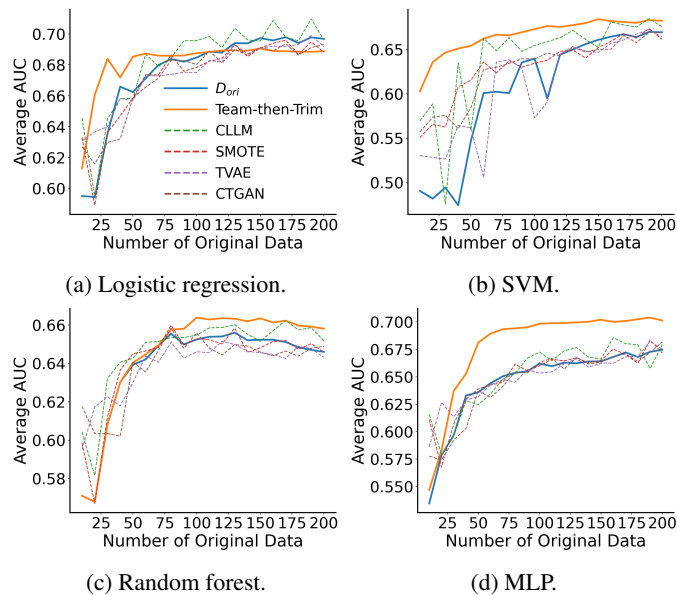
1019 **Model utility.** Fig. 10 presents the average AUC of four ML models trained on the augmented
 1020 COMPAS dataset across varying sizes of original data from 10 to 200. Across all models, team-then-
 1021 trim outperforms baseline approaches under most sizes of original data. Importantly, while classical
 1022 baselines occasionally achieve moderate gains, their improvements are inconsistent and often fall
 1023 short of the stability achieved by team-then-trim. These trends indicate that the coordinated LLM-
 1024 teaming plus trimming pipeline enhances model utility in ways that benefit a broad spectrum of
 1025 downstream learners.

1026

1027

1028 Table 7: Average performance (%) across different sizes of D_{ori} (from 10 to 100) when data is noisy
1029 in the diabetes data.
1030

Flip Ratio	Method	AUC	F1	Recall
0.2	D_{ori}	79.00	73.26	75.13
	SMOTE	78.73	70.81	75.90
	TVAE	77.47	72.32	75.35
	CTGAN	75.38	72.99	74.07
	CLLM	77.99	68.70	68.91
	Team-then-Trim w/o QC	80.83	71.10	72.39
	Team-then-Trim	81.42	72.62	74.84
	D_{ori}	64.42	64.66	67.41
	SMOTE	69.77	63.03	69.57
	TVAE	63.67	64.76	70.21
0.3	CTGAN	66.44	62.87	68.65
	CLLM	69.96	61.16	61.88
	Team-then-Trim w/o QC	70.99	63.41	65.69
	Team-then-Trim	71.84	64.78	67.69
	D_{ori}	59.18	58.34	58.91
0.4	SMOTE	62.66	59.17	59.53
	TVAE	61.52	56.72	57.82
	CTGAN	57.40	54.20	55.23
	CLLM	63.86	60.64	49.73
	Team-then-Trim w/o QC	66.61	58.12	58.48
	Team-then-Trim	65.94	58.95	59.76

1076 Figure 10: Average AUC of four ML models across original data from 10 to 200 on COMPAS
1077 dataset.
1078
1079

1080 Table 8: **Token usage and runtime cost of LLM-based data generation under the Diabetes (Imbal-**
 1081 **anced) setting.**

1082

Method	Components	Tokens (Input)	Tokens (Output)	Time (s)
CLLM	–	771	872	6.56
Team-then-Trim	LLM Worker 1	832	387	4.83
	LLM Worker 2	1831	887	6.08
	LLM Worker 3	2457	1483	7.16
	LLM Worker 4	2533	1507	7.46

1083

1090 E EXAMPLE: THE ADVANTAGE OF LLM TEAMING

1091

1092 Fig. 11 presents generated data examples from a single LLM and from LLM teaming on COMPAS
 1093 dataset. The feature “juv_fel_count” denotes the number of juvenile felonies of a defendant, while
 1094 “priors_count” represents the total number of prior criminal records. By definition, “priors_count”
 1095 should always be greater than or equal to “juv_fel_count”. As shown in Fig. 11a, data generated by
 1096 a single LLM fails to respect this rule, whereas in Fig. 11b, our proposed LLM teaming framework
 1097 successfully produces data that adheres to such basic consistency constraints.

1098

juv_fel_count	juv_misd_count	juv_other_count	priors_count	juv_fel_count	juv_misd_count	juv_other_count	priors_count
2	0	0	0	1	0	1	2
3	0	1	2	0	1	3	4
...				...			

1100

(a) Single LLM.

1101

(b) LLM teaming.

1102

1103 Figure 11: **Comparison of generated data on COMPAS from a single LLM and the proposed LLM**
 1104 **teaming framework.**

1105

1106

1107 F LLM USAGE

1108

1109

1110 We employ LLMs to generate tabular data as part of our framework. Beyond this, all written content
 1111 in this paper is authored by us. After completing the draft, we use LLMs to assist with grammar
 1112 checking.

1113

1114

1115

1116

1117

1118

1119

1120

1121

1122

1123

1124

1125

1126

1127

1128

1129

1130

1131

1132

1133